Koga, D., Gonjo, T., Kawai, E., Tsunokawa, T., Sakai, S., Sengoku, Y., Homma, M., Takagi, H. (2020). Effects of exceeding stroke frequency of maximal effort on hand kinematics and hand propulsive force in front crawl. *Sports Biomechanics*. https://doi.org/10.1080/14763141.2020.1814852

Effects of exceeding stroke frequency of maximal effort on hand kinematics and hand propulsive force in front crawl

Daiki Koga[a], Tomohiro Gonjo[b], Eisuke Kawai[c], Takaaki Tsunokawa[a], Shin Sakai[a], Yasuo Sengoku[a], Miwako Homma[a] and Hideki Takagi[a]

[a]*Faculty of Health and Sport Sciences, University of Tsukuba, Tsukuba, Ibaraki, Japan*

[b]*Department of Physical Performance, Norwegian School of Sport Sciences, Oslo, Norway*

[c]*Faculty of Physical Education, International Budo University, Katsuura, Chiba, Japan*

E-mail

Corresponding author

Hideki Takagi: takagi.hideki.ga@u.tsukuba.ac.jp

ORCiDs

Daiki Koga: https://orcid.org/0000-0001-9429-3331

Tomohiro Gonjo: http://orcid.org/0000-0001-9118-5167

Eisuke Kawai: https://orcid.org/0000-0003-1847-977X

Miwako Homma: https://orcid.org/0000-0002-0531-4696

Hideki Takagi: http://orcid.org/0000-0001-8797-7014

Word count: 4153

Effects of exceeding stroke frequency of maximal effort on hand kinematics and hand propulsive force in front crawl

This study aimed to assess kinematic and kinetic changes in front crawl with various stroke frequency (*SF*) conditions to investigate why swimming velocity (*SV*) does not increase above a certain *SF* (SF_{max}). Eight male swimmers performed 20 m front crawl four times. The first trial involved maximal effort, whereas *SF* was controlled during the next three trials. The instructed *SF*s were 100 (*T*100%), 110 (*T*110%), and 120% (*T*120%) of the SF_{max}. Through pressure measurement and underwater motion analysis, hand propulsive force (calculated by the difference between the palm and dorsal pressure value and the hand area) and the angle of attack of the hand were quantified, and differences between trials were assessed by a repeated-measures ANOVA. There was no difference in *SV* between the conditions, while the angle of attack during the latter half of the underwater stroke at *T*120% was smaller by 25.7% compared with *T*100% (p = 0.007). The lower angle of attack induced a lower pressure value on the palm that consequently caused a smaller hand propulsive force at *T*120% than *T*100% (p = 0.026). Therefore, the decrease in the angle of attack must be minimised to maintain the hand propulsive force.

Keywords: swimming velocity; fluid dynamics; motion analysis; motor; angle of attack

Introduction

Swimmers propel themselves forward using upper and lower limbs. In front crawl, the contribution by the upper limbs to propulsive force is greater than that of the lower limbs (Deschodt, Arsac, & Rouard, 1999). However, it is difficult to accurately assess the propulsive force exerted by the upper limbs because the direct measurement of the hydrodynamic profile around the entire limbs has not been established. In recent years, a method has been developed to estimate the propulsive force by measuring the pressure distribution around the hand and foot directly using water-proof pressure sensors (Tsunokawa, Tsuno, Mankyu, Takagi, & Ogita, 2018; Tsunokawa, Nakashima, & Takagi, 2015; Kawai, Tsunokawa, & Takagi, 2018).

Takagi and Wilson (1999) examined the validity of the hand propulsive force calculated by measuring the pressure distribution at the hand during sculling with various weight load on the swimmers. They calculated the pressure differences between the palm and dorsal side at four points on the hand using eight pressure sensors and estimated the mean pressure difference between the palm and the dorsal sides of the entire hand using a regression equation. Then, they calculated the hand fluid force by multiplying the hand area. The hand propulsive force was defined as a vertical component of the hand fluid force, and a high positive correlation was observed between the hand propulsive force and added weight load ($r = 0.986$, $p < 0.001$). This result suggested a good validity of the method.

On the other hand, since the approach developed by Takagi and Wilson was a method to assess the hydrodynamic forces during sculling motion, Kudo, Yanai, Wilson, Takagi, & Vennell (2008) established a method of estimating the fluid force during front crawl upper limb motion using pressure distribution at 12 points on the hand. They reported that their method estimated the fluid force with a root mean square error of 5 N. This method has an advantage in predicting not only the force components toward the direction perpendicular to the hand but also the directions parallel to the hand plane. However, since the pressure sensors are wired, using a large number of sensors might disturb the upper limb motion of the swimmer, and many wires might alter the flow pattern around the upper limbs.

Tsunokawa et al. (2018) adapted the method of Takagi and Wilson (1999) using a small number of sensors, which reduced the aforementioned risks. The pressure differences between the palm and the dorsal side of three points of a hand were measured using six pressure sensors, and the fluid force was estimated by multiplying the pressure difference on each point by a corresponding hand segment area. With this method, it has been reported that the hand propulsive force rises with the increase in swimming velocity (*SV)* (Tsunokawa, Mankyu, Takagi, & Ogita, 2019), underpinning that the hand propulsive force is an important factor to achieve large *SV*.

From a kinematic perspective, *SV* is determined by stroke frequency (*SF*) and stroke length (*SL*). Therefore, when swimmers improve either or both parameters, they increase *SV*. However, it has been reported that a long training period is required to improve *SL* (Wakayoshi, Yoshida, Ikuta, Mutoh, & Miyashita, 1993). Conversely, Seifert, Chollet, & Bardy (2004) have demonstrated a positive correlation between *SF* and *SV* when the swimmers swam in the *SV* of 3000 m, 1500 m, 800 m, 400 m, 200 m, 100 m, 50 m and maximal (r = 0.92, p < 0.05). Therefore, *SF* contributes more to an increase in *SV* in a short period of time than *SL*. On the other hand, another study suggested that *SV* does not increase when the *SF* exceeded the *SF* of maximal effort swimming (SF_{max}) (Craig & Pendergast, 1979). Craig and Pendergast (1979) suggested that a high *SF* above SF_{max} could be achieved by placing the hand close to the water surface to reduce the force exerted by the hand. Nakashima, Maeda, Miwa, and Ichikawa (2012) also reported that the angle of attack of the hand was decreased with the reduction of stroke time using a human swimming simulation model (SWUM), and they suggested that this was particularly the case in the latter half of the underwater stroke. However, these results are based on a computer simulation, and it is unclear whether these phenomena are also the case in actual swimmers.

At sprint swimming, swimmers start the latter half of the stroke from the angle of attack of 50-60° and the angle gradually decreases to around 20° with an average value of 37-38° (Samson, Monnet, Bernard, Lacouture, & David, 2015; Samson, Monnet, Bernard, Lacouture, & David, 2018b). Van Houwelingen, Schreven, Smeets, Clercx, and Beek (2017) reviewed the relationship between drag coefficient, lift coefficient, and angle of attack in steady-state in three numerical studies and five experimental studies. The review noted that most studies showed no noticeable differences in results, and swimmers show the highest drag and lift coefficient around the angle of attack of 90° and 50°, respectively. Samson, Monnet, Bernard, Lacouture, and David (2018a) calculated these values in unsteady-state using Computational Fluid Dynamics (CFD) to consider unsteady state and concluded that the lift and drag coefficients were highest at angles of attack of 40-60° and 80-90°, respectively. This means that if the angle of attack becomes smaller than 40° above SF_{max}, it will probably reduce the force acting on the hand.

Therefore, it was hypothesised that *SV* does not change or decreases when *SF* exceeds SF_{max} because a decrease in the angle of attack during the latter half of the stroke causes a reduction in the hand propulsive force. This study aimed to investigate changes in the hand propulsive force and the angle of attack using the hand propulsive force estimation and kinematic analysis in front crawl in various high *SF* conditions to establish why *SV* does not increase above SF_{max}.

Materials and methods

Participants

Eight male swimmers participated in the present study (Table 1). All participants were right-handed. The University of Tsukuba Research Ethics Committee approved the procedure and potential risks in this study. Prior to the testing, all participants were informed about the procedures and risks of the study and written informed consent forms were obtained from each of them.

(Table 1)

Experimental design

Before the trials, the participants conducted a self-selected warm-up. Thereafter, they performed four times 20 m front crawl between 5 and 25 m from the pool wall without breathing. They started with a floating position to minimise the effect of wall push-off on *SV*. The first trial was their maximal effort (*Max*), and the next three trials were maximal effort swimming with controlled *SF*. The *SF* of *Max* was defined as SF_{max}, and 100%, 110% and 120% of SF_{max} were calculated and used for the next three trials (*T*100%, *T*110% and *T*120%). The trial order was from *T*100% to *T*120% in a progressive order with at least three minutes rest between trials. In a preliminary experiment, the swimmers were asked to try the trials with a random order, and some of them had difficulty with achieving the instructed *SF* (especially at *T*120%), whereas all swimmers could follow the *SF* instruction with the progressive order. Therefore, the progressive order was selected to minimise the risk of swimmers failing many trials and the effect of fatigue on the results. In the three trials with *SF* instruction, the swimmers followed the sound of an electronic metronome (Tempo Trainer Pro, FINIS Inc.) so that they could coordinate their *SF* to the instructed frequency. Immediately after each trial, *SF* was obtained as the average of *SFs* during three stroke cycles using video footage. If *SF* was within ±2.5% of the instructed *SF*, the trial was considered to be acceptable, whereas the trial was repeated if the *SF* was beyond ±2.5%. The swimmers practised swimming with the electronic sound metronome to swim with *SF* higher than SF_{max} at least twice a week for three weeks to familiar with the protocol.

Data acquisition

Light-emitting diode wireless active markers (Nobby Tech. Ltd., Japan) were attached to the right acromial, the right second and fifth metacarpophalangeal (MP), the right radial styloid process, and the right ulnar styloid process. The three-dimensional (3D) global coordinates of the markers during the trials were recorded using a 3D real-time motion analysis system VENUS 3D (Nobby Tech. Ltd., Japan) with a sampling frequency of 100 Hz. A 3D direct linear transformation method with dynamic calibration was used. The range of calibrated area was 5-m long between 17 and 22 m from the pool wall, and 15 waterproof motion capture cameras were placed in the water surrounding the area (Figure 1). The standard error of underwater motion capture calibration was less than 0.3 mm. A right-hand fixed coordinate system was used, with the *X*-axis as the right and left direction, the *Y*-axis as the forward direction and the *Z*-axis as the vertical direction (Figure 1). The origin of the coordinate system was the centre of the measurement range on the *X*-axis, the 20 m point from the wall on the *Y*-axis, and the water surface on the *Z*-axis.

(Figure 1).

To measure the pressure distribution on the surface of a swimmer's hand during the trials, six small waterproof pressure sensors (PS-05KC, Kyowa Electronic Instruments Co. Ltd., Japan) were used according to the method of Tsunokawa et al. (2018). These sensors measure only the pressure component acting perpendicular to the sensor and cannot measure the force of the friction component. However, Samson, Monnet, Bernard, Lacouture, & David (2017) reported that the main contributor to the propulsive force was the pressure component (pressure vs friction at the latter half of the stroke: 25.4 N vs -0.4 N). Therefore, it was assumed that the pressure component would represent the force produced by the hand. These sensors were attached on the palm and dorsal sides of the second, third and fifth metacarpophalangeal joints (Figure 1). The signal output from the pressure sensors was recorded on a laptop with 100 Hz using a universal recorder (EDX-100A, Kyowa Electronic Instruments Co. Ltd., Japan). All signals from the motion capture system and the pressure sensors were synchronised and stored on the computer. The pressure sensors were wired; therefore, a trolley carrying the equipment was moved along with the swimmer on the pool deck. One stroke cycle of front crawl was defined from an entry of the right hand to the subsequent entry of the same hand. Due to the limited range of the data collection, only one stroke cycle performed within the calibrated area was analysed.

Data processing

The mean *SV* was calculated by differentiating the distance the swimmer travelled in the *Y*-axis direction during one stroke cycle by the time (Matsuda, Sakurai, Akashi, & Kubo, 2018). *SF* was the inverse of the time taken for one stroke cycle, and *SL* was calculated by dividing the mean *SV* by *SF*. Mean hand speed was the resultant speed of the midpoint of the hand markers during the underwater stroke. Mean angle of attack during the underwater stroke was calculated as the angle between the hand velocity vector and the hand plane which was composed of two vectors pointing from the right ulnar styloid process to the fifth MP joint and the second MP joint.

Pressure sensors measured both hydrodynamic and hydrostatic pressures. Hydrostatic pressure was calculated from water density (1000 kg/m^3), gravitational acceleration (9.8 m/s^2), and depth and extracted from the data. In this study, the depth of each pressure sensor was calculated from the coordinates of the second and fifth MP joints and mid-point of the two joints. The hydrodynamic pressure was filtered using a low-pass Butterworth filter with 20 Hz cut-off frequency according to the method of Tsunokawa et al. (2018). The filtered hydrodynamic pressure was calculated as a palm and dorsal pressure value during the underwater stroke duration.

The underwater stroke motion was divided into the following phases: the glide phase, which is the period from the point where the *Z* coordinate of the fifth MP joint is zero until the point at which the *Y* coordinate of the fifth MP joint starts to move backwards; the pull phase, which is the period from the end of the glide phase until the *Y* coordinate of the fifth MP joint reaches below the *Y* coordinate of the acromion; and the push phase, which is the period from the end of the pull phase until the *Z* coordinate of the fifth MP becomes zero. Based on these phases, angle of attack, hand speed, phase time, each pressure value, hand fluid force, and hand propulsive force were calculated for each phase. In the phase time, the time above water was also calculated.

Calculation of hand propulsive force

The plane of the hand was divided into three sections by the second and fourth interdigital spaces (Figure 1). The pressures differences between the palm and dorsal pressure value at each segment was considered as the representative hydrodynamic pressure at each segment. The hand fluid force was calculated by multiplying the dynamic pressure of each segment by the area of each segment, and the overall hand fluid force was obtained by summing the hand fluid forces calculated at each segment (Tsunokawa et al., 2018, 2019). The area of the right hand segments was determined by manually tracing the hand shape on a graph paper with 5 mm grid, which was divided into each segment, and then summing all 25 mm^2 squares included in the segment.

This method derives the hand fluid force perpendicular to the hand plane. Thus, the normal vector to the hand plane was defined as the direction of the vector of the hand fluid force. Since the estimated hand fluid force is the resultant force acting on the hand, the force was divided into three components (*X*, *Y* and *Z*). In this study, we defined the force in the *Y*-axis direction as the hand propulsive force (Tsunokawa et al., 2018). While the hand was above the water, it was defined that the hand fluid force and hand propulsive force was not exerted. The mean value of hand fluid force and hand propulsive force were calculated as the mean of one stroke cycle.

Statistical analysis

Statistical processing was conducted using IBM SPSS Statistics 25.0 (IBM, USA). The normality of data was verified using the Shapiro-Wilk normality test and confirmed in all variables. In order to test differences in calculated variables between trials, a one-way repeated measures ANOVA was conducted. When the main effect was observed, multiple comparisons were conducted using a paired t-test with the Bonferroni adjustment. A *p*-value of <0.05 was considered to be statistically significant.

Results

Mean value of one stroke cycle and underwater stroke duration

Table 2 present the mean values of each parameter in one stroke cycle and underwater stroke duration. *SF* significantly increased as instructed (F [2,14] = 209.4, $p < 0.001$). The hand speed also increased significantly (F [2,14] = 209.4, $p < 0.001$). No significant differences were observed in *SV*. *SL* significantly decreased (F [2,14] = 130.6, $p = 0.001$) between each trial as *SF* increased. The palm pressure value significantly decreased (F [2,14] = 8.7, $p = 0.004$). The hand propulsive force was also significantly decreased (F [2,14] = 8.9, $p = 0.003$). There were no significant differences in dorsal pressure value, the hand fluid force, and the angle of attack between each trial. *SV* did not change significantly at *T*110% compared with *T*100%. However, one swimmer decreased *SV*, and three swimmers achieved higher *SV* and hand propulsive force at *T*110% than at *T*100% (Table 3).

(Table 2)

(Table 3)

Mean values of each of the three phases in underwater strokes

Figure 2 and 3 present the mean values of each parameter in the three phases (glide, pull and push). The angle of attack significantly decreased in the push phase (F [2,14] = 8.9, p = 0.003) (Figure 2a). The hand speed significantly increased in the glide phase (F [2,14] = 11.1, p = 0.001) and the push phase (F [2,14] = 19.8, p < 0.001) (Figure 2b). With increasing *SF*, phase time was significantly reduced in the glide phase (F [2,14] = 36.1, p < 0.001), in the the push phase (F [2,14] = 7.5, p = 0.006) and above water (F [2,14] = 24.3, p < 0.001) (Figure 2c). The palm pressure value significantly decreased in the push phase (F [2,14] = 26.2, p < 0.001) (Figure 3a). The dorsal pressure value significantly decreased in the glide phase (F [2,14] = 5.9, p = 0.014) (Figure 3b). In the push phase, the hand fluid force significantly decreased (F [2,14] = 11.7, p = 0.001) (Figure 3c). Similarly, the hand propulsive force significantly decreased in the pull phase (F [2,14] = 11.0, p = 0.001) and in the push phase (F [2,14] = 17.8, p < 0.001) (Figure 3d).

(Figure 2)

(Figure 3)

Discussion and implication

The purpose of this study was to investigate why *SV* does not increase above SF_{max} from both kinematic and kinetic perspectives. It has been reported that *SV* and the hand propulsive force increase with the increment in *SF* (Tsunokawa et al., 2019). On the other hand, other studies have suggested that *SV* does not change or decreases when *SF* increases above SF_{max}; however, the reason for this was unclear (Craig & Pendergast, 1979; Nakashima et al., 2012; Nakashima & Ono, 2014). Our results showed that the angle of attack in the push phase and the mean hand propulsive force were lower at *T*120% compared with *T*100%. Interestingly, *SV* was similar between *T*100% and *T*120% despite the decrease in the mean propulsive force, which might be related to the increase in *SF*. In front crawl swimming, a rise in *SF* causes an increase in the overlap of the left-right propulsive phases (Chollet, Chalies, & Chatard, 2000; Sifert et al., 2004), which might have compensated for the decrease in the propulsive force in one stroke cycle. However, this study did not analyse left and right upper limb coordination; accordingly, this should be investigated in future studies.

The hand propulsive force reduction during the push phase at *T*120% was caused by a decrease in the angle of attack. The hand propulsive force is a propulsive direction component of the hand fluid force. The propulsive component of the force decreases when the hand fluid force decreases or the rate of the propulsive force component relative to the total force decreases due to a change in the hand orientation. In this study, the fluid force acting perpendicular to the hand was estimated. Given that swimmers primarily move their hand backwards during the underwater stroke, it is reasonable to conclude that the change in the angle of attack is directly related to the change in the hand orientation relative to the swimming direction that is linked to the rate of the propulsive force component.

Since the hand fluid force is the pressure difference between the palm and the dorsal sides, a decrease in the palm pressure value or an increase in the dorsal pressure value results in a decrease in the pressure difference. The palm pressure value is affected by the angle of attack. When the angle of attack is large, the angle of the main flow vector to the palm is close to vertical to the hand plane, and the palm pressure value perpendicular to the hand increases (Figure 4, left). Conversely, when the angle of attack is small, the hand plane moves almost parallel to the main flow vector (Figure 4, right), thereby the palm pressure value perpendicular to the hand decreases. At *T*120%, the pressure component of the main flow vector perpendicular to the hand plane decreases due to the decrease in the angle of attack. On the other hand, the dorsal pressure value did not change with the angle of attack. Previous studies implied that the dorsal pressure value is related to wake structure and flow speed on the dorsal side (Dickinson, 1996; Samson et al., 2018a). Even though the flow speed on the dorsal side probably increased with the increment in the hand speed, no change in dorsal pressure value was observed. Therefore, the difference in the wake structure due to the difference in the angle of attack might have influenced the dorsal pressure value. Using CFD method, Samson et al. (2018a) showed that vortices with different patterns were observed on the dorsal side when changing the angle of attack, and they implied that the vortices are linked to the pressure on the dorsal side. This evidence supports the possibility of the effect of the wake structure on the dorsal pressure value in this study. However, the flow field around the hand was not measured in this study and the direct evidence supporting this possibility is currently lacking. Further research is necessary to investigate the effect of the angle of attack as well as *SF* on the dorsal pressure values.

(Figure 4)

It is important to maintain the angle of attack when *SF* is increased because a decrease in the angle of attack is the primary factor of the hand propulsive force reduction. However, maintaining the optimal angle of attack with a high hand speed would probably produce a large drag force that opposes to the hand, meaning that increasing hand speed and maintaining the angle of attack are somewhat contradictory. Especially, as hand speed in push phase is the highest velocity among underwater stroke phase, adjusting the hand fluid force acting on the hand by decreasing the angle of attack was probably a solution for the swimmers to achieve high instructed *SF*. In other words, during maximal effort swimming, swimmers use an angle of attack that allows them to exert their maximum hand propulsive force and the highest hand speed that can be maintained with a proper angle of attack to produce the drag or lift force. Therefore, to improve the maximum *SV* of swimmers by increasing their *SF*, it is necessary to conduct training at higher *SF* than SF_{max} of the swimmers so that they can maintain the same angle of attack as SF_{max} condition. Since the stroke movement is a complex movement involving not only the upper limb motion but also the trunk and upper limb cyclic motions (Sanders & Psycharakis, 2009), it is also necessary to ensure the entire movements being well-coordinated when prescribing such training to swimmers.

At *T*120%, almost all the participants showed a decrease in *SV* and the hand propulsive force compared with the values at *T*110% (although not all changes were statistically significant in *SV*), implying that the *SF* at *T1*20% was too high to aim for a higher *SV* than at *T*110%. Conversely, three swimmers achieved higher *SV* at *T*110% than at *T*100%, and their hand propulsive force was also higher (Table 3). In other words, the subjective maximum effort is not necessarily the same as the effort that allows the swimmer to achieve the fastest *SV*, and some swimmers could potentially achieve a higher *SV* than their subjective maximum effort swimming by increasing their *SF*. Therefore, it is necessary for swimmers to try various *SF* in their training, including *SF* higher than their maximum effort to occasionally ascertain the optimal *SF* to achieve the fastest *SV*.

Limitations

The present study has some limitations. This investigation involved the hand propulsive force and hand kinematics under the assumption of the hand propulsive force being the primary source of the total propulsive force produced by the upper limbs. The pressure sensors used in this study could only measure the pressure acting in a direction perpendicular to the hand plane. Given that the main contributor to propulsive force is the pressure component perpendicular to the hand (Samson et al., 2017), estimation of propulsive force from hand surface pressure distribution measurements is probably reasonable. However, propulsive forces are also generated by the forearm and upper arm.

Hence, there is a possibility that our results were affected by kinematics and kinetics of these segments. In the latter half of underwater stroke, the contribution of the pressure component on the forearm to propulsion is smaller than that of the hand (about 25%) (Samson et al., 2017). The low pressure component is possibly due not only to the difference in the shape of the segments but also to the increase in the contribution of the friction component to the propulsion force due to the generation of axial flow from the shoulder to the hand (Toussaint & Beek, 2002). Therefore, it is necessary to measure the friction component in the future to measure the propulsive force accurately.

Conclusion

Swimmers decreased the angle of attack in the push phase (the latter half of the underwater stroke), which caused a decrease in the hand propulsive force during this phase. Consequently, the mean hand propulsive force decreased, and *SV* did not change despite the increase in *SF*. Therefore, it is important to maintain the angle of attack during the push phase to prevent the decrease in the hand propulsive force when increasing *SF*.

Acknowledgements

We are grateful to all the members of the Swimming Laboratory at the University of Tsukuba for their helpful advice. In addition, the authors would like to thank the executive committee members of KEIHIROBA group in the Japanese Society of Biomechanics for their insightful comments.

Funding details

None.

Disclosure statement

The authors have no potential conflict of interest to declare.

References

Chollet, D., Chalies, S., & Chatard, J. C. (2000). A new index of coordination for the crawl: description and usefulness. *International journal of sports medicine, 21*(01), 54-59. doi: 10.1055/s-2000-8855

Craig, A.B., & Pendergast, D.R. (1979). Relationships of stroke rate, distance per stroke, and velocity in competitive swimming. *Medicine and Science in Sports*, *11*, 278–283.

Deschodt, J.V., Arsac, L.M., & Rouard, A.H. (1999). Relative contribution of arms and legs in humans to propulsion in 25-m sprint front-crawl swimming. *European Journal of Applied Physiology, 80*, 192–199. doi: 10.1007/s004210050581

Dickinson, M.H. (1996). Unsteady mechanisms of force generation in aquatic andaerial locomotion. *American Zoologist*. *36* (6), 537–554. doi:10.1093/icb/36.6.537

Kawai, E., Tsunokawa, T., & Takagi, H. (2018). Estimating the hydrodynamic forces during eggbeater kicking by pressure distribution analysis. *Heliyon*, *4*(12), e01095. doi: 10.1016/j.heliyon.2018.e01095

Kudo, S., Yanai, T., Wilson, B., Takagi, H., & Vennell, R. (2008). Prediction of fluid forces acting on a hand model in unsteady flow conditions. *Journal of Biomechanics*, *41*(5), 1131-1136. doi: org/10.1016/j.jbiomech.2007.12.007

Matsuda, Y., Sakurai, Y., Akashi, K., & Kubo, Y. (2018). A practical estimation method for center of mass velocity in swimming direction during front crawl swimming. *Journal of Applied Biomechanics*, *34*, 342–347. doi: 10.1123/jab.2017-0188

Nakashima, M., Maeda, S., Miwa, T., & Ichikawa, H. (2012). Optimising simulation of the arm stroke in crawl swimming considering muscle strength characteristics of athlete swimmers. *Journal of Biomechanical Science and Engineering*, *7*, 102–117. doi: 10.1299/mej.17-00377

Nakashima, M., & Ono, A. (2014). Maximum joint torque dependency of the crawl swimming with optimised arm stroke. *Journal of Biomechanical Science and Engineering*, *9*, JBSE0001. doi: 10.1299/jbse.2014jbse0001

Samson, M., Monnet, T., Bernard, A., Lacouture, P., & David, L. (2015). Kinematic hand parameters in front crawl at different paces of swimming. *Journal of Biomechanics, 48,* 3743–3750. doi: 10.1016/j.jbiomech.2015.07.034

Samson, M., Monnet, T., Bernard, A., Lacouture, P., & David, L. (2017). Unsteady computational fluid dynamics in front crawl swimming. *Computer Methods in Biomechanics and Biomedical Engineering*. *20* (7), 783–793. doi:10.1080/10255842.2017.1302434

Samson, M., Monnet, T., Bernard, A., Lacouture, P., & David, L. (2018a). Analysis of a swimmer's hand and forearm in impulsive start from rest using computational fluid dynamics in unsteady flow conditions. *Journal of Biomechanics*. *67*, 157–165. doi: 10.1016/j.jbiomech.2017.12.003

Samson, M., Monnet, T., Bernard, A., Lacouture, P., & David, L. (2018b). Comparative study between fully tethered and free swimming at different paces of swimming in front crawl. *Sports Biomechanics*. *18*(6): 571-586. doi: 10.1080/14763141.2018.1443492.

Sanders, R. H., & Psycharakis, S. G. (2009). Rolling rhythms in front crawl swimming with six-beat kick. *Journal of Biomechanics*, *42*(3), 273-279. doi: 10.1016/j.jbiomech.2008.10.037

Seifert, L., Chollet, D., & Bardy, B.G. (2004). Effect of swimming velocity on arm coordination in the front crawl: a dynamic analysis. *Journal of Sports Sciences*, *22*, 651–660. doi:10.1080/02640410310001655787

Takagi, H., & Wilson, B., (1999). Calculating hydrodynamic force by using pressure differences in swimming. In K. Keskinen, P. Komi & A.P. Hollander (Ed.), *Biomechanics and Medicine in Swimming VIII* (pp.101-106). Gummerus Printing Jyvaskyla.

Toussaint, H. M., & Beek, W. J. (2002). " Pumped-up propulsion" during front crawl swimming. *Medicine and science in sports and exercise*, *34*(2), 314-319. doi: 10.1097/00005768-200202000-00020

Tsunokawa, T., Mankyu, H., Takagi, H., & Ogita, F. (2019). The effect of using paddles on hand propulsive forces and Froude efficiency in arm-stroke-only front-crawl swimming at various velocities. *Human Movement Science*, *64*, 378–388. doi: 10.1016/j.humov.2019.03.007

Tsunokawa, T., Nakashima, M., & Takagi, H. (2015). Use of pressure distribution analysis to estimate fluid forces around a foot during breaststroke kicking. *Sports Engineering*, *18*(3), 149-156. doi: 10.1007/s12283-015-0174-6

Tsunokawa, T., Tsuno, T., Mankyu, H., Takagi, H., & Ogita, F. (2018). The effect of paddles on pressure and force generation at the hand during front crawl. *Human Movement Science*, *57*, 409–416. doi: 10.1016/j.humov.2017.10.002

Van Houwelingen, J., Schreven, S., Smeets, J. B., Clercx, H. J., & Beek, P. J. (2017). Effective propulsion in swimming: grasping the hydrodynamics of hand and arm movements. *Journal of applied biomechanics*, *33*(1), 87-100. doi: 10.1123/jab.2016-0064

Wakayoshi, K., Yoshida, T., Ikuta, Y., Mutoh, Y., & Miyashita, M. (1993). Adaptations to six months of aerobic swim training. Changes in velocity, stroke rate, stroke length and blood lactate. *International Journal of Sports Medicine*, *14*, 368–372. doi: 10.1055/s-2007-10211

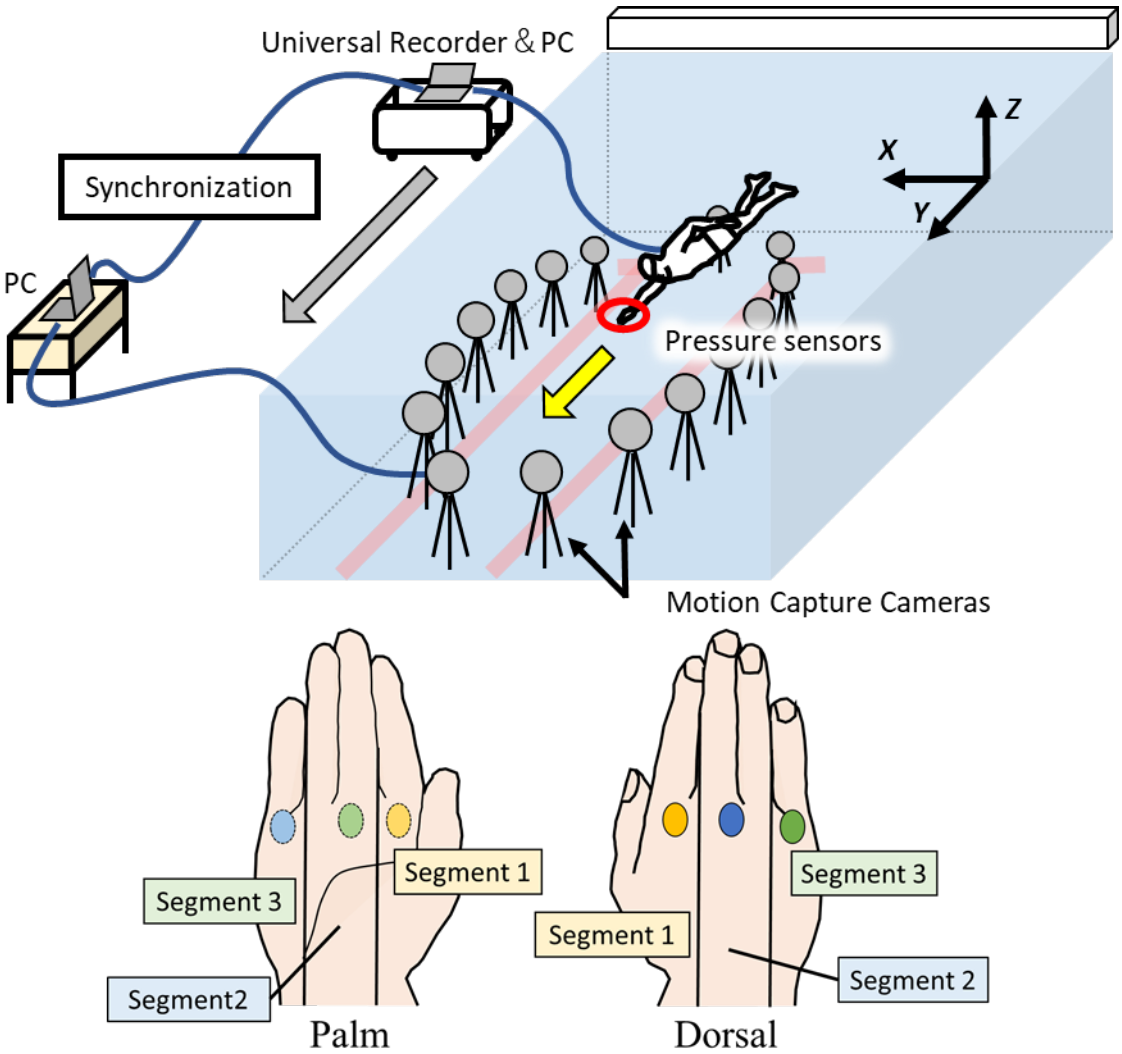

Figure 1. Experimental setting and the location of the pressure sensors attached to the hand.

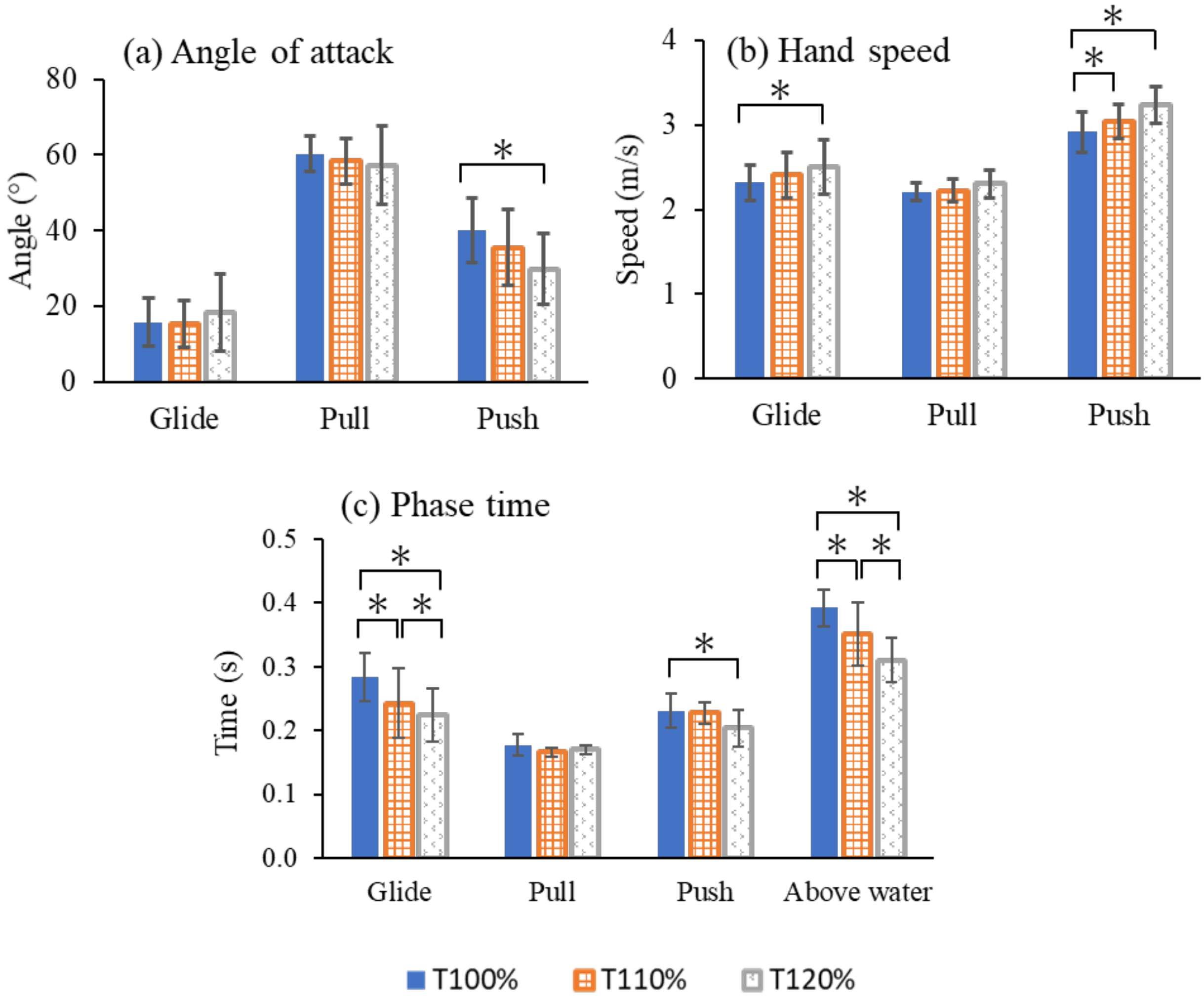

Figure 2. Angle of attack, hand speed, and phase time in each phase at different trials. (*: $p < 0.05$)

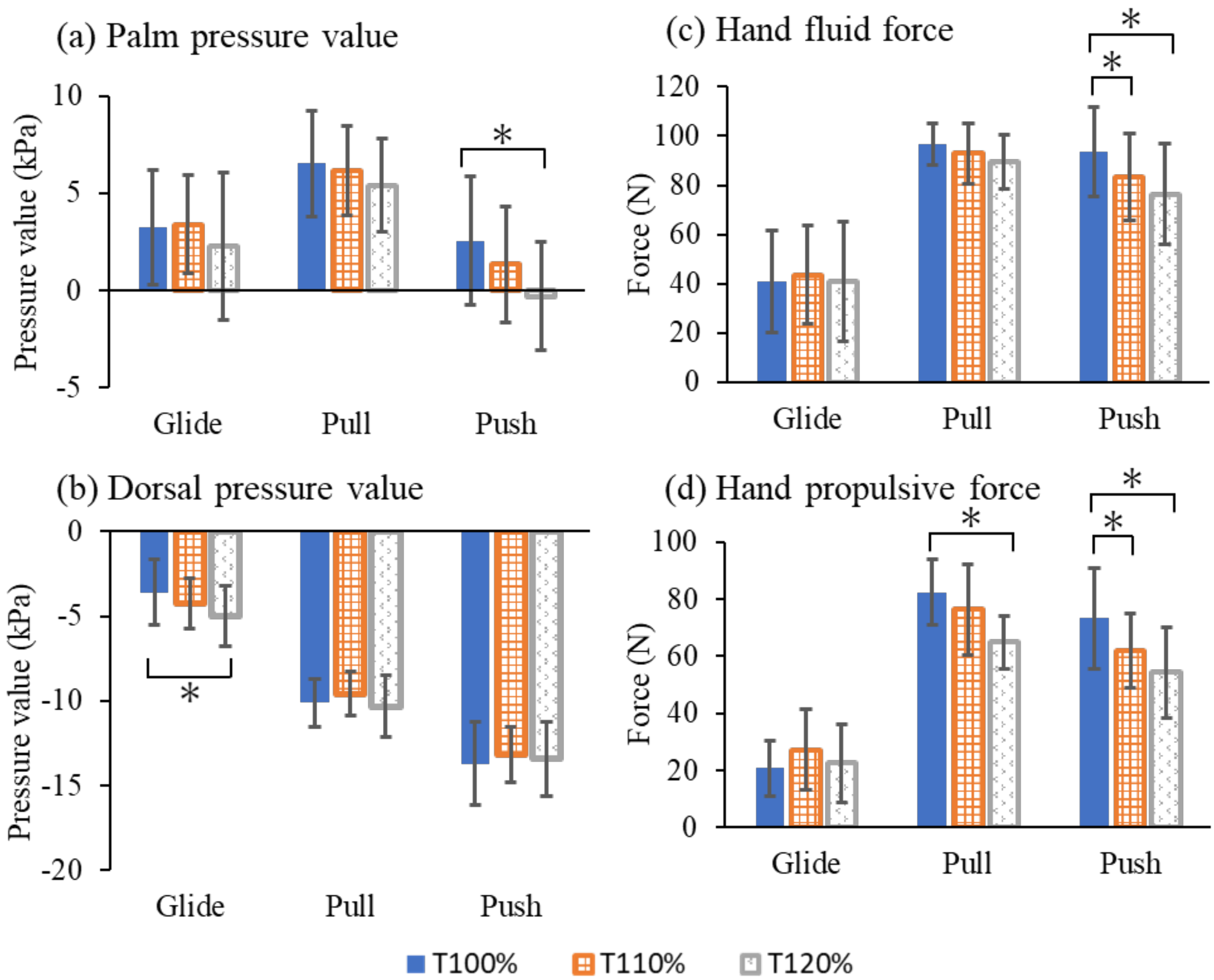

Figure 3. Palm pressure value, dorsal pressure value, hand fluid force, and hand propulsive force in each phase at different trials. (*: $p < 0.05$)

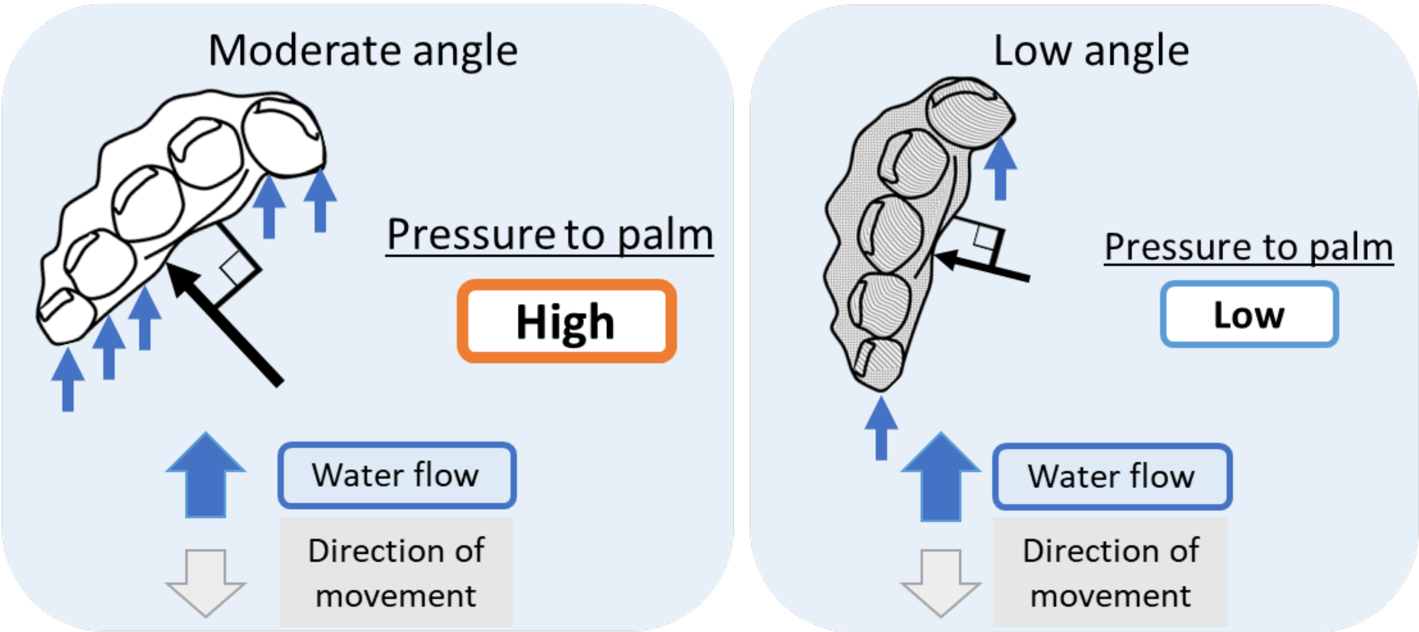

Figure 4. Image of moderate (left) and low (right) angle of attack.

Table 1. Physical characteristics and swimming performance of the study participants.

Swimmer	Age (years)	Height (m)	Weight (kg)	Specialty	Best Record of 50 m front crawl (s)	Fina Point
A	23	1.84	81.0	Front crawl	22.74	777.5
B	24	1.84	81.0	Front crawl	22.96	755.3
C	23	1.78	82.5	Front crawl	23.19	733.1
D	20	1.77	80.0	Front crawl	23.35	718.1
E	20	1.87	80.0	Front crawl	23.37	716.3
F	23	1.86	84.0	Front crawl	23.80	678.2
G	20	1.83	77.0	Front crawl	24.26	640.3
H	20	1.75	76.0	Individual Medley	24.31	636.4
mean	21.6	1.82	80.2		23.50	706.9
SD	1.7	0.04	2.5		0.54	48.0

Table 2. Mean values of variables during one stroke cycle of each parameter.

	*T*100%	*T*110%		*T*120%	
Swimming velocity (m/s)	1.75 ± 0.06	1.76 ± 0.07		1.74 ± 0.07	
Stroke frequency (stroke/s)	0.93 ± 0.05	1.01 ± 0.05	a	1.11 ± 0.06	ab
Stroke length (m/stroke)	1.89 ± 0.08	1.73 ± 0.07	a	1.57 ± 0.08	ab
Hand speed (m/s)	2.49 ± 0.16	2.58 ± 0.15		2.69 ± 0.19	ab
Palm pressure value (kPa)	2.88 ± 2.22	2.78 ± 2.17		2.05 ± 2.45	ab
Dorsal pressure value (kPa)	-8.90 ± 1.31	-9.39 ± 1.64		-9.10 ± 1.59	
Hand fluid force (N)	46.0 ± 8.9	45.6 ± 10.3		43.3 ± 10.3	
Hand propulsive force (N)	34.1 ± 5.8	33.9 ± 6.2		29.7 ± 7.4	ab
Angle of attack (°)	34.8 ± 4.1	34.0 ± 3.6		33.3 ± 5.0	

a: Significant difference when compared to *T*100%, b: Significant difference when compared to *T*110%.

Table 3. Mean swimming velocity and mean hand propulsive force of the participants at *T*100%, *T*110% and *T*120%.

The grey mesh shows the participants whose mean swimming velocity and mean hand propulsive force increased more in the *T*110% than in the *T*100%.

Swimmer	*Swimming velocity* (m/s)			*Hand propulsive force* (N)		
	*T*100%	*T*110%	*T*120%	*T*100%	*T*110%	*T*120%
A	1.82	1.83	1.83	41.3	40.7	40.0
B	1.80	1.83	1.82	38.6	39.0	36.8
C	1.86	1.94	1.87	32.5	37.3	31.1
D	1.74	1.70	1.66	41.6	38.6	34.1
E	1.73	1.73	1.70	26.5	22.2	18.5
F	1.66	1.66	1.63	29.1	32.4	21.7
G	1.70	1.70	1.70	34.4	32.1	26.6
H	1.66	1.68	1.67	29.1	29.3	28.8
mean	1.75	1.76	1.74	34.1	33.9	29.7
SD	0.06	0.07	0.07	5.8	6.2	7.4